Available online at www.sciencedirect.com
ScienceDirect
Geomorphology 87 (2007) 16–27
GEOMORPHOLOGY
www.elsevier.com/locate/geomorph

Modelling the location of shallow landslides and their effects on landscape dynamics in large watersheds: An application for Northern New Zealand

L. Claessens [a,b,*], J.M. Schoorl [a], A. Veldkamp [a]

[a] Laboratory of Soil Science and Geology, Wageningen University and Research Centre, P.O. Box 37, 6700 AA Wageningen, The Netherlands
[b] International Potato Center (CIP), Sub-Saharan Africa Regional Office, P.O. Box 25171, 00603 Nairobi, Kenya

Received 19 May 2003; received in revised form 20 June 2006; accepted 20 June 2006
Available online 18 September 2006

Abstract

In this study we propose a model to assess the location of shallow landslides and their impact on landscape development within a timeframe of years to decades. Processes that need to be incorporated in the model are reviewed then followed by the proposed modelling framework. The capabilities of the model are explored through an application for a forested 17 km^2 study catchment in Northern New Zealand for which digital elevation data are available with a grid resolution of 25 × 25 m. The model predicts the spatial pattern of landslide susceptibility within the simulated catchment and subsequently applies a spatial algorithm for the redistribution of failed material by effectively changing the corresponding digital elevation data after each timestep on the basis of a scenario of triggering rainfall events, relative landslide hazard and trajectories with runout criteria for failed slope material. The resulting model will form a landslide module within the dynamic landscape evolution model LAPSUS. The model forms a spatially explicit method to address the effects of shallow landslide erosion and sedimentation because digital elevation data are adapted between timesteps and on- and off-site effects over the years can be simulated in this way. By visualization of the modelling results in a GIS environment, the shifting pattern of upslope and downslope (in) stability, triggering of new landslides and the resulting slope retreat by soil material redistribution due to former mass movements can be simulated and assessed.

Keywords: Shallow landslides; Slope instability; Catchment model; Erosion; Deposition

1. Introduction

Shallow landslides are one of the most common types of landslides, occurring frequently in steep, soil mantled landscapes in different climatic zones (e.g. Kirkby, 1987; Benda and Cundy, 1990; Selby, 1993). In many cases, failure and transport of slope material by landsliding is one of the principal processes of soil redistribution and hillslope development in landscapes.

Landslides have traditionally been regarded as key indicators of forest disturbance, particularly in association with logging activities (Douglas, 1999; Douglas et al., 1999; Montgomery et al., 2000; Fannin and Wise, 2001), land use and climatic change (Van Beek, 2002; Vanacker et al., 2003) or as response to human imposed changes such as road building (Brand and Hudson, 1982; Larsen and Torres-Sanchez, 1998). Over the past decades most model studies dealing with landslides have mainly focussed on landslide hazards and terrain

* Corresponding author. International Potato Center (CIP), Sub-Saharan Africa Regional Office, P.O. Box 25171, 00603 Nairobi, Kenya. Tel.: +254 20 422 3612; fax: +254 20 422 3001.
E-mail address: l.claessens@cgiar.org (L. Claessens).

0169-555X/$ - see front matter © 2006 Elsevier B.V. All rights reserved.
doi:10.1016/j.geomorph.2006.06.039

stability mapping for regional and urban planning (Van Westen, 1993; Guzzetti et al., 1999) and the impact of landslides on basin sediment yield (Burton and Bathurst, 1998). Also a number of recent landslide studies have been concerned with identifying rainfall thresholds required to trigger landslide events (Crozier, 1999) or magnitude and frequency of landsliding in a specific catchment (Reid and Page, 2003). However, as a mass movement process, rainfall-triggered landslides have been underestimated as contributors to slope development and denudation in the past (Dykes, 2002). Geomorphological investigations in steeplands show evidence that shallow landslides play a key role in the maintenance of characteristic slope forms and probably also make significant contributions to ecological dynamics (Dykes and Thornes, 1996; Claessens et al., 2006).

At present relatively few attempts have been made to model the effects of shallow landslides on landscape development. Modelling the relevant processes in a dynamic way requires a methodology aggregating several mechanisms acting at different spatial and temporal scale levels but remaining at least spatially explicit over a timeframe concerning redistribution of soil material. Kirkby (1987) identifies two major difficulties in the context of models of longer term landscape development: work on rapid mass movements has concentrated on stability analysis, so that forecasting of destinations for slide debris is very inexact, even for an individual slide. Modelling of slope profile evolution is severely restricted by a lack of studies on the factors controlling travel distances of mobilized material, which are crucial to the development of an overall mass budget in a forecasting context. The second major problem lies in aggregating from the individual slide to the assemblage of slides over a long period wherefore detailed meteorological records are generally not available. The change of temporal scale requires models that are built from somewhat different premises than those used for short-term stability analysis, although obviously they must be compatible.

The practical significance of shallow landsliding has motivated many approaches of mapping and predicting potential landslide initiation (for a review see Montgomery and Dietrich, 1994). A recent approach, which is proven to be very practical, is the use of digital elevation models and simple coupled hydrological and slope stability models (Dietrich et al., 1992, 1993; Montgomery and Dietrich, 1994; Wu and Sidle, 1995; Borga et al., 1998; Pack et al., 2001; Borga et al., 2002). Availability of GIS technology permits then to resolve and display spatial patterns of landslide susceptibility at the same scale and resolution as the digital terrain model.

In general landslides triggered on forested slopes release such energy and mass that a debris flow nearly always develops. This flow erodes the unstable material in its path and continues to move downslope until the gradient falls below that needed to maintain flow (Burton and Bathurst, 1998). To study the role of rainfall-induced landslides within the hierarchy of hillslope erosion processes on the longer term, it is therefore important not only to know the spatial distribution of possible landslide initiation sites but also to characterize erosion and deposition patterns caused by slope failure. Removal of failed landslide material can potentially increase the local slope by taking away initial support and may trigger subsequent upslope failure. Additional downslope erosion and failure may occur along the debris flow erosional pathway and by loading and steepening downslope material by debris flow deposition. Once a debris flow emerges, the problem of determining its path becomes complicated by the ability of the flow to erode, to spread, to plug, and to alter its direction. The rate of volume transport of a debris flow and its change with time, viscosity and hillslope morphology are some factors important for debris flow erosion and deposition.

Using data from individual events, two-dimensional mathematical models for flows on fans have been calibrated to determine flow depths, velocities, impact forces and areas of deposition (Mizuyama and others, 1987; Mizuyama and Ishikawa, 1990; O'Brien and Fullerton, 1990; Takahashi, 1991). These methods require a large amount of data along with numerous assumptions about the characteristics of the debris flow. Formulations from laws of mass and momentum conservation are complex and more appropriate for examination of the detailed behaviour of an individual debris flow for which the flow material composition and hillslope characteristics are well specified (Bathurst et al., 1997). For our goal a simpler, rule-based and spatially explicit approach is used that can easily be applied to multiple landslides occurring throughout a catchment over periods of time ranging from single rainstorms to several years and for which the data specification is more general.

2. Materials and methods

2.1. Study area

The Waitakere Ranges Regional Parkland lies immediately west of Auckland city, New Zealand (174.8 °E, 36.9 °S, Fig. 1). It is mostly covered in thick virgin and regenerating native forest and popular for wilderness activities and tramping. Most of the land is publicly owned, forming part of Auckland Centennial Memorial

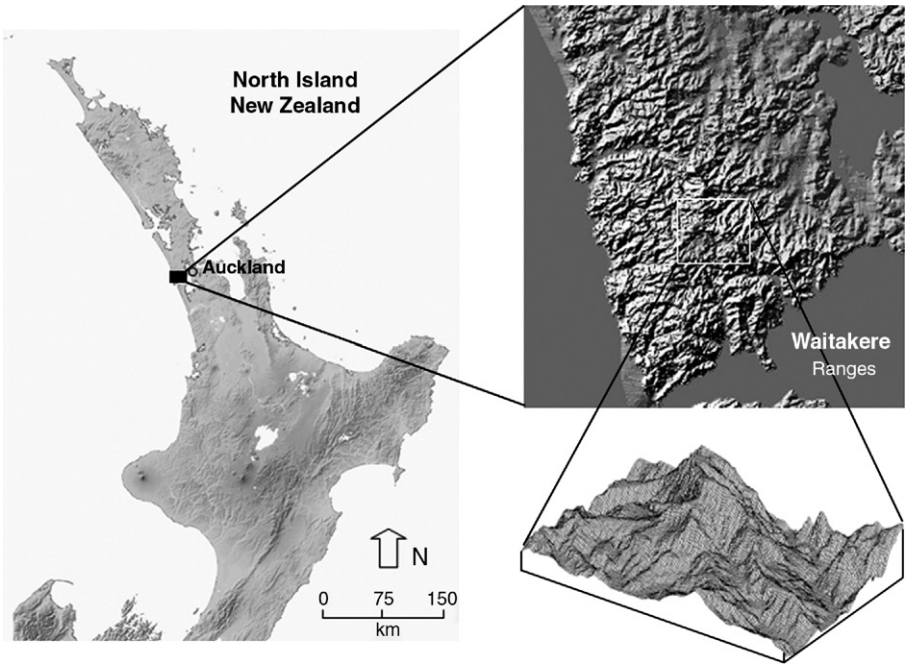

Fig. 1. Study area location within New Zealand and 3D representation of the Waitakere Ranges.

Park and water catchment land with restricted entry. Altitude ranges from sea level to 474 m.

The area has a warm and humid subtropical climate with a mean annual rainfall ranging from about 1400 mm near the Tasman coast up to 2030 mm at the higher altitudes (ARC, 2002). Daily rainfall data from 1988–2003 are available from two climate stations in Swanson and at the Arataki visitor's centre. A Magnitude-Frequency Index (MFI) for daily rainfall totals of the study area is calculated according to Ahnert's (1987) method (Fig. 2. This results in a MFI of 60.0; 10.7, meaning a daily rainfall of 60 mm is reached or exceeded once a year and a daily rainfall of 70.7 mm or more occurs once every ten years.

The rugged topography of the area is caused by the resistant nature of the component rocks. The ranges are formed predominantly of Miocene volcanic breccia and conglomerate (Piha Formation), andesitic to basaltic lava flows (Lone Kauri Formation) and well-bedded volcanic sandstone and siltstone (Nihotupu Formation) (Hayward,

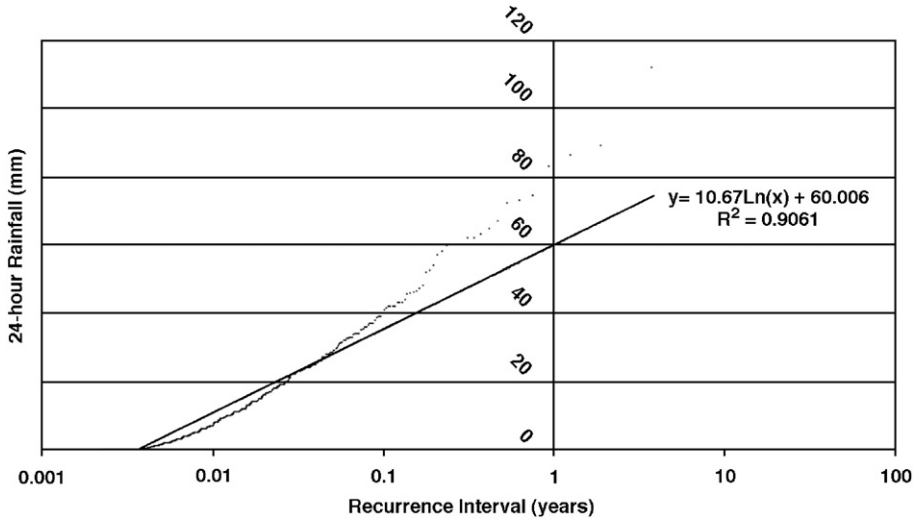

Fig. 2. Magnitude-Frequency plot for daily rainfall totals measured at the Arataki visitor centre 1988–2003.

1976). The topography is entirely erosional; none of the original volcanic landforms are preserved. In general the landscape is mantled by very deep soils but locally bedrock crops out on steep side slopes, in cliffs, volcanic dikes and intrusions. Soils are classified as haplic Acrisols according to the FAO classification (FAO, 2001). The clay composition of the soils is dominated by kaolinite but varying fractions of smectite, halloysite and vermiculite clays are present.

The Waitakere Ranges have a history of human modification and use extending back less then one thousand years. Especially in the previous century timber milling has modified the area drastically. Farming also resulted in extensive areas being cleared of their original vegetation. With the development of a water supply system for Auckland with reservoir lakes and dams and to ensure the purity of this water supply 2610 ha of forest was retired from development and allowed to recover naturally (Murdoch, 1991). By now 8882 ha have some form of protection and are mostly covered in thick virgin and regenerating native forest (Denyer et al., 1993).

Shallow landsliding is an important sediment transport process in the ranges, especially on steep side slopes and in topographic hollows. Slope failure is most common in soils developed in the weak sandstone and siltstone of the Nihotupu Formation but also frequently occurs in the weathered volcanic breccias and lava flows of the Piha and Lone Kauri Formation. Slope failures involving 1 to 40 m^3 of soil material are common within moderately to highly weathered rock (particularly the finer grained materials), on slopes steeper than 18 ° in cleared areas and on slightly steeper slopes in bush covered areas (Hayward, 1983).

2.2. Modelling framework

The modelling environment for embedding the shallow landslide component is comprised by the landscape evolution model LAPSUS (*L*andsc*A*pe *P*roces*S* modelling at m*U*lti dimensions and scale*S*) (Schoorl et al., 2000). This approach is a finite element model based on early works of Kirkby (1971) and Foster and Meyer (1972, 1975). It addresses on-site and off-site effects of current and possible water and soil redistribution by water run-off and tillage erosion. Landscape evolution within a timeframe of decades is simulated in a dynamic way by adapting digital elevation data between yearly timesteps according to calculated soil redistribution. The model was developed for a well documented cultivated area in the Mediterranean climate zone of Southern Spain. Calibration of the model was done with the ^{137}Cs technique and different land use scenarios were applied to yield changes in erosion and sedimentation patterns (e.g. Schoorl and Veldkamp, 2001; Schoorl et al., 2002). For application in the New Zealand catchment, where shallow landsliding is the most dominant soil redistribution process, a new landslide component is added to the existing model structure. A complete integration of all the model components for broader application, dealing with the erosion and sedimentation processes caused by water run-off, tillage erosion and shallow landsliding is foreseen.

2.3. Landslide hazard modelling

Montgomery and Dietrich (1994), based on earlier formulations proposed by O'Loughlin (1986), combined a contour based steady state hydrologic model with a deterministic infinite slope stability model to delineate areas prone to landsliding due to surface topographic effects on hydrologic response. Our approach is based on this method but has two differences (as in Pack et al., 2001):

1) The cohesion term is retained in the infinite slope stability model to account for differences in soil cohesion between geological formations and additional strength by root reinforcement for different vegetation types.
2) We use grid-based rather than contour based DEM methodology.

The infinite slope stability model factor of safety is defined as the ratio of the available shear strength (stabilizing forces) to the shear stress (destabilizing forces) (e.g. Graham, 1984). With soil depth interpreted as specified perpendicular to the slope surface, rather than measured vertically, the factor of safety (FS) can be written as (Pack et al., 2001):

$$FS = \frac{\left(C + \cos\theta\left[1 - W\left(\frac{\rho_w}{\rho_s}\right)\right]\tan\phi\right)}{\sin\theta} \quad (1)$$

where C is combined cohesion [–], W is a relative wetness index [–], θ is local slope angle [°], ρ_s wet soil bulk density [g/cm^3], ρ_w the density of water [g/cm^3] and ϕ is the effective angle of internal friction of the soil [°]. The combined cohesion term C is made dimensionless relative to the perpendicular soil thickness and is defined as follows:

$$C = \frac{C_r + C_s}{h\rho_s g} \quad (2)$$

where C_r is root cohesion [N/m^2], C_s is soil cohesion [N/m^2], h is perpendicular soil thickness [m] and g is the gravitational acceleration constant (9.81 m/s^2). C is thus the ratio of total cohesive strength relative to the soil depth or can be interpreted as the relative contribution to slope stability of the cohesive forces. W is the relative wetness, which is the ratio of local flux at a given steady state rainfall to that at soil profile saturation. For the calculation of W in our application, we use a steady state hydrologic response model based on the work by O'Loughlin (1986) and Moore et al. (1988) in which W can be defined as:

$$W = \frac{Ra}{bT\sin\theta} \tag{3}$$

with R is the steady state rainfall recharge [m/d], a is the upslope contributing drainage area [m^2], b is the unit contour length, T is the soil transmissivity when saturated [m^2/d] and θ is the local slope angle [°]. For b, grid size [m] is taken as the effective contour length, independent upon flow direction as in Pack et al. (2001). Wetness cannot exceed 1 because any excess is assumed to form overland flow. Hence the range of values for W is between 0 and 1. By substituting Eq. (1), equating the factor of safety to 1, which is the threshold for instability, and solving for R we can determine the minimum steady state rainfall predicted to cause slope failure. We call Q_{cr} [m/d] the critical rainfall, which can be written as:

$$Q_{cr} = T\sin\theta\left(\frac{b}{a}\right)\left(\frac{\rho_s}{\rho_w}\right)\left[1-\frac{(\sin\theta - C)}{(\cos\theta\tan\phi)}\right] \tag{4}$$

With the boundary conditions for W (between 0 and 1), we can express the conditions for upper and lower thresholds for elements that can possibly fail according to Eq. (4). Unconditionally stable areas are predicted to be stable, even when saturated and have:

$$\tan\theta \leq \left(\frac{C}{\cos\theta}\right) + \left(1-\frac{\rho_w}{\rho_s}\right)\tan\phi \tag{5}$$

Unconditionally unstable elements, which are bedrock outcrops in most cases, are unstable even when dry and have:

$$\tan\theta > \tan\phi + \left(\frac{C}{\cos\theta}\right) \tag{6}$$

In the model, local slope and wetness are calculated at each grid point and the other parameters are lumped within an area of same parent material and vegetation type. In this way the spatial distribution of critical rainfall values can be calculated as an expression of the potential for shallow landslide initiation. The upslope contributing drainage area used in the calculation of W is calculated using the concept of multiple downslope flow (Quinn et al., 1991) to represent the convergence or divergence of flow under topographic control.

2.4. Trajectories of failed slope material

Most of the empirical approaches found in literature try to quantify the impact of shallow landslides on sediment yield at the catchment scale. Bathurst et al. (1997) tested, both with hypothetical hillslopes and field data, four empirical models for determining percentage delivery of sediment to streams for shallow landslides that evolve into debris flows. The best compromise between simplicity and reliability proved to be a model based on a study by Vandre (1985), which is also used by Burton and Bathurst (1998). In the model, debris flow runout distance R [m] is expressed as:

$$R = \varphi\Delta y \tag{7}$$

where Δy [m] is the elevation difference between the head of the slide and the point at which deposition begins (this point is reached once the gradient falls below a certain slope angle) and φ [−] is an empirically derived fraction set at 0.4 (Vandre, 1985; Burton and Bathurst, 1998). For our approach the use of the elevation loss within the erosional phase as a measure of debris flow momentum at the start of deposition is adapted from this method. However the runout distance itself, originally aimed at quantifying percentage sediment delivery to streams, is treated differently. The trajectory of the depositional phase is not routed following the steepest descent nor is the debris flow material spread uniformly over the full runout distance. Instead, the importance of hillslope morphology for the spatial deposition pattern is incorporated by using a combination of multiple flow routing principles and R as a measure for the reach of downslope gridcells receiving material in the depositional phase.

The way soil material is redistributed in our model is as follows: in the erosional phase, the debris flow accumulates unstable soil material following the steepest descent gradient. Johnson and Rodine (1984) express the critical thickness of debris flow material z [m] beginning to flow or stop flowage on an infinite slope depending on local slope and soil geotechnical properties according to:

$$z = \frac{C_s}{\rho_s\cos\theta(\tan\theta - \tan\phi')} \tag{8}$$

in which ϕ' is the apparent or bulk angle of internal friction, including the effect of pore water pressure as debris flow initiation mechanism. In this way, flow is impossible if the bulk friction angle is equal to or greater than the slope angle, that is if $\phi' \geq \theta$. Often approximations of a minimum slope gradient for maintaining flow are used (e.g. Ikeya, 1981; Johnson and Rodine, 1984; Benda and Cundy, 1990; Wu and Sidle, 1995; Burton and Bathurst, 1998). We propose to put such a slope limit on debris flow movement by inversing Eq. (8), substitute ϕ' by a slope angle limit for debris flow movement and estimate the amount of eroded material S [m] depending on soil geotechnical properties and local gradient as:

$$S = \frac{\rho_s \cos\theta(\tan\theta - \tan\alpha)a}{C_s} \quad (9)$$

where α [°] is the minimum local slope for debris flow movement and a [m^2] is a correction factor for dimensions. In this way, the amount of eroded material is regarded as inversely proportional to the minimal depth for debris flow mobilization (substituting the bulk internal friction angle ϕ' by a slope limit α). On steeper slopes and for less cohesive soils, more material is eroded.

The point at which deposition begins or where the added erosion material reduces to zero is then reached once the gradient falls below a certain slope angle α (e.g. 10°, depending on the typical landslide dimensions of the area). At this point we define the number of downslope gridcells involved in the deposition of debris flow material as 'cell-distance' D [–] and this is calculated as:

$$D = \left(\frac{R}{b}\right) \quad (10)$$

where R is the debris flow runout distance as defined in Eq. (7) and b is the gridcell resolution [m]. The accumulated soil material is than further routed with a 'double' multiple flow methodology as illustrated in Fig. 3. For downslope neighbours of the point where deposition starts we can express the sediment, which is effectively delivered to gridcell n as:

$$S_n = \left(\frac{B_{n-1}}{D_{n-1}}\right) f \quad (11)$$

The term B_{n-1}/D_{n-1} is the amount of sediment coming from upslope divided by the cell-distance and being deposited in gridcells n. The remaining sediment

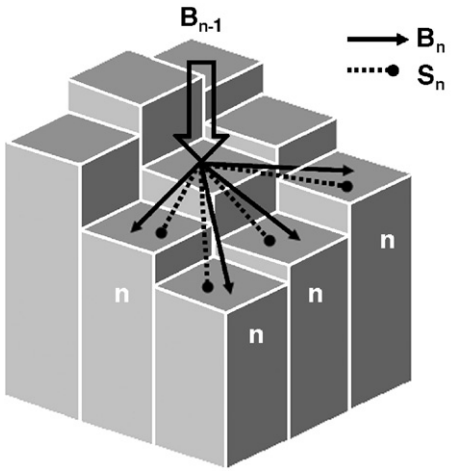

Fig. 3. Schematic representation of the 'double' multiple-flow methodology. Further explanation is in the text.

budget of gridcell n, which is not delivered but passed through to gridcells $n+1$ can be expressed as:

$$B_n = B_{n-1}\left(1 - \frac{1}{D_{n-1}}\right) f \quad (12)$$

In both Eqs. (11) and (12) f is the fraction of sediment (S) either sediment budget (B) allocated to each lower neighbour and determined by the multiple flow algorithm by Quinn et al. (1991). In each downslope grid step, the cell-distance is then lowered by 1:

$$D_n = D_{n-1} - 1 \quad (13)$$

When $D < 1$ all the remaining sediment is deposited and the debris flow halts.

2.5. Input data

Field data of the study area were obtained during systematic field surveys carried out from March to May 2002. To test the predictive power of the landslide hazard model an inventory of shallow landslide features was made. Shallow landslides involving just the soil mantle are very common and form the main erosional features in the area. However, due to the dense vegetation in the steep canyon areas, it is difficult to map all the scars, even in the field. Some of the scars are probably several decades old based on the vegetation cover and sharpness of the edges. Using a time series of aerial photography and field inspection with a GPS device we mapped 76 landslide scars in the study area. The scars

Table 1
Soil physical model input parameters for the three parent materials

Formation	C_s [kPa]±S.E.	ϕ [rad]±S.E.	ρ_s [g/cm^3]	T [m^2/d]
Piha	5.976±1.946	0.678±0.029	1.447	18
Lone Kauri	12.223±2.157	0.688±0.032	1.455	15
Nihotupu	13.352±2.140	0.548±0.032	1.436	11

Table 2
Combined cohesion values for combinations of the three parent materials and the four vegetation classes

Formation	C [–] Kauri	C [–] Podocarp/ Broadleaf	C [–] Broadleaf	C [–] Successional
Piha	0.42	0.37	0.30	0.26
Lone Kauri	0.64	0.59	0.52	0.48
Nihotupu	0.69	0.63	0.56	0.53

are most commonly encountered on the steeper footslopes and at the downstream end of small steep, unchanneled valleys.

Soil properties are strongly related to the parent material. Therefore soil physical parameters used in the model are assumed to be uniform within geological units. Digitising of areas with the same parent material was done according to the 1:50 000 geological map of New Zealand, sheet Q11 (Hayward, 1983). Transmissivity values are estimated on the basis of field measurements of saturated hydraulic conductivity using the inversed augerhole method (Kessler and Oosterbaan, 1974). Saturated bulk densities of the three soil types were determined in the laboratory (Table 1). Saturated shear strength of the soil material has been determined by consolidated-drained direct shear tests on undisturbed samples taken from soils developed in the three main parent materials of the area. The undisturbed blocks of clay taken in the field were trimmed to fit inside a shearbox with dimensions 10×10×2.5 cm. The samples were subjected to normal loads of 28–95 kPa. Results are shown in Fig. 4 and Table 1.

Root strength of both tree and understory vegetation provides significant apparent cohesion to the soil. To address the relative importance of different vegetation types in increasing the resistance against shallow landsliding by root reinforcement, a vegetation classification was needed. A survey for the Protected Natural Areas Programme (Denyer et al., 1993) yielded a detailed vegetation map of the Waitakere ecological district. We used this map as a basis to delineate and assign root cohesion values to four main vegetation classes occurring in the catchment. Back analysis of slope failures mapped in the field and by aerial photography interpretation made it possible to calibrate the model for our application by adapting the root cohesion in the combined cohesion term for each vegetation class. The apparent cohesion values attributed to the different vegetation classes are well within range of the results obtained by other researchers (e.g. Selby, 1993; Montgomery et al., 2000; Dykes, 2002). An overview of all combined cohesion values per vegetation class and parent material is given in Table 2.

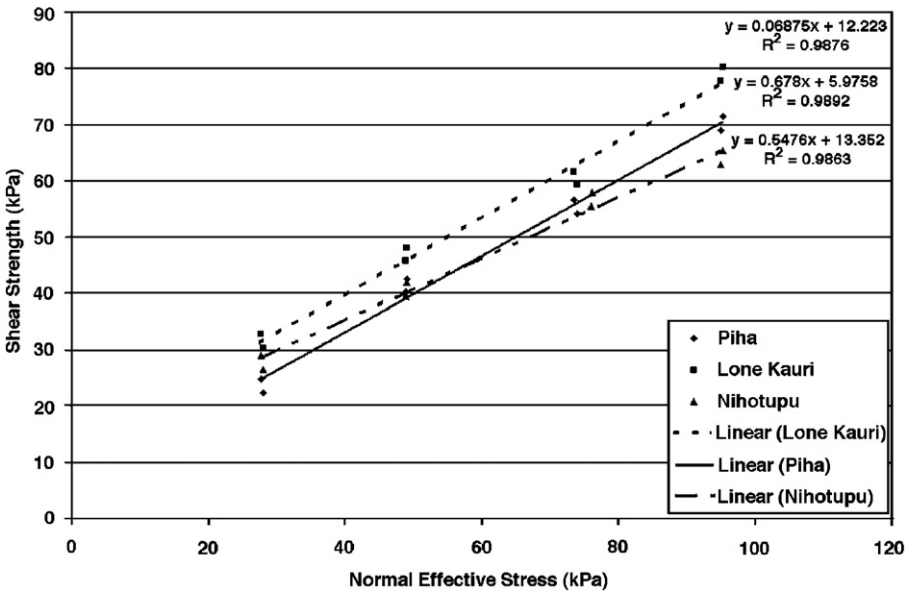

Fig. 4. Shear strength envelopes for soils developed in the three main parent materials.

Digital elevation data for the Waitakere Ranges were available with a 25 × 25 m grid resolution (see Fig. 1). To obtain a hydrologically sound DEM, both sinks and pits, whose height is lower than that of all their connected neighbours, were removed by increasing the elevation of to that of the lowest point in the pit perimeter. The local slope was derived from the DEM and the upslope contributing drainage area was computed using the multiple flow algorithm of Quinn et al., 1991.

3. Results and discussion

3.1. Application for Waitakere Ranges catchment

To explore the performance and sensitivity of the described method the model is applied to a forested 17 km^2 catchment within the Waitakere Ranges, which is well documented and comprises all the variability in parent material and vegetation types. We parameterised the model based on field observations and measurements of the input parameters according to Tables 1 and 2 and tested the ability of the model to explain the spatial and temporal patterns of shallow landsliding over a longer time period. A realistic scenario for the occurrence of landslide triggering rainstorms with a certain intensity was applied to each timestep of one decade based on long term rainfall records in combination with back analysis of detected landslides on time series of aerial photographs. The model calculates for each timestep the relative potential for sliding and, according to the scenario, redistributes landslide material of failed sites following the transport trajectories described above. After each timestep the digital elevation data are adapted according to these debris flow erosion and deposition patterns.

Because the shallow landsliding in the study area is not weathering — but transport limited we do not have to take soil production rates into account. Although it has been shown and recognized that both geotechnical and hydrological behaviour are altered as regolith is stripped from hillsides and redeposited on footslopes (Brooks et al., 2002) we assume here that sites which failed in one timestep regain their full relative potential for sliding, i.e. their original soil physical parameter setting, in the subsequent timestep. An overview map with visualizations of the regions of debris flow erosion and deposition is shown in Fig. 5 and a more detailed area is represented in Fig. 6. When we run the model for several consecutive timesteps it is possible to compare the different landslide hazard maps between the timesteps and get insight in the pattern of upslope and downslope triggering of new landslides and the resulting slope retreat. Fig. 7 shows a detail of the landslide hazard maps produced after timestep one and five. Important spatial shifts in landslide hazards can be noted. After the occurrence of a slide, higher hazards are found upslope the failed slide due to undercutting and steepening of the slope above the eroded part. Also downslope of the failure, parts with a higher landslide potential are encountered caused by steepening of local slopes mainly on the sides of the landslide sediment lobe. Because water from upslope is more canalized towards the steepened eroded part of the landslide, the contributing area of the areas bordering the channel is reduced, thereby lowering failure potential. In this way the model simulates the mosaic-like shifting pattern of upslope and downslope triggering of new landslides over years by soil material redistribution due to former mass movements.

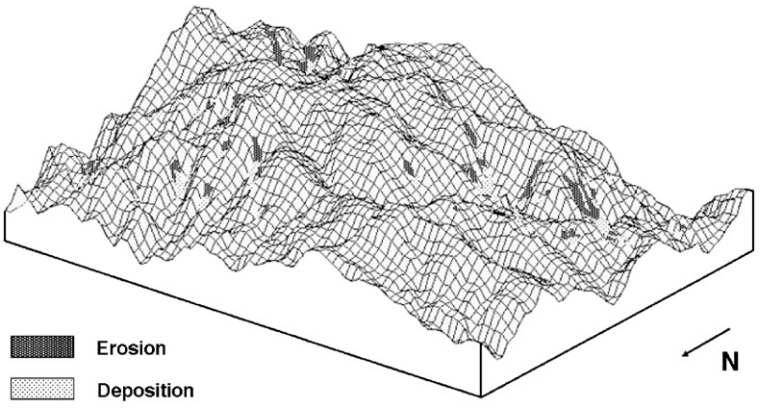

Fig. 5. Landslide erosion- and deposition patterns for failures with a critical steady state rainfall of 25 mm/day or less. Note that the DEM is displayed in another resolution than that of the model output.

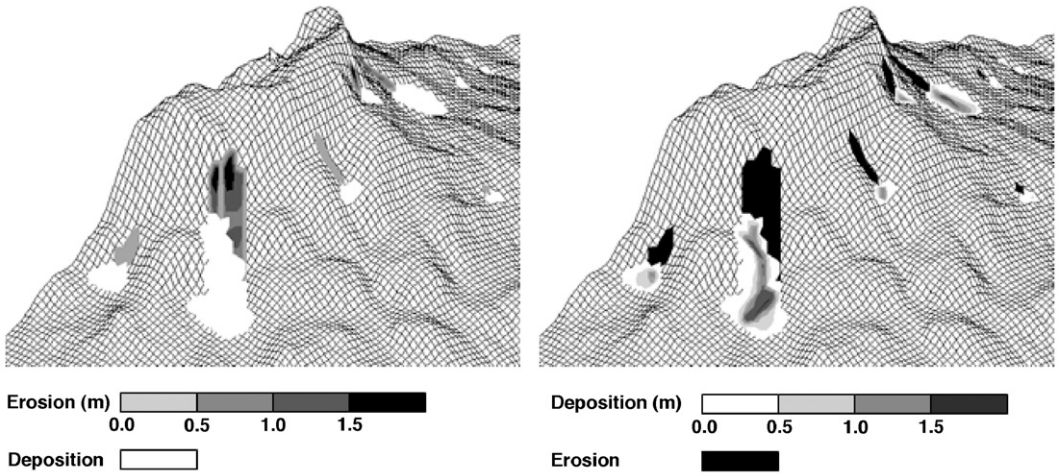

Fig. 6. Detail of landslide erosion- and deposition patterns.

3.2. Model validity

Several assumptions have been made in model development and parameterisation. The use of C as a dimensionless parameter in the factor of safety calculation is convenient but it implies that a constant soil thickness is assumed. Another assumption in the wetness calculation is that saturated hydraulic conductivity, and therefore also transmissivity, do not vary with depth. If a spatially distributed varying soil depth is taken into account, soil production functions should be used and hydraulic conductivity might vary with depth (Dietrich et al., 1995). The steady state hydrologic model requires the assumption that the predicted spatial pattern of landslide hazard under a critical steady state rainfall represents that which occurs during an unsteady, landslide producing rainfall event. Furthermore the relative potential for shallow landslides is supposed to be determined by convergence of shallow subsurface flow, following the surface topography and proportional to the upslope contributing area. The small velocity of subsurface flow might prevent a reliable application of the steady state assumption and it is likely that most points receive contributions from only a small proportion of their total upslope contributing area. In general, the notion of critical rainfall should only be considered as a relative measure of failure potential (Borga et al., 1998, 2002).

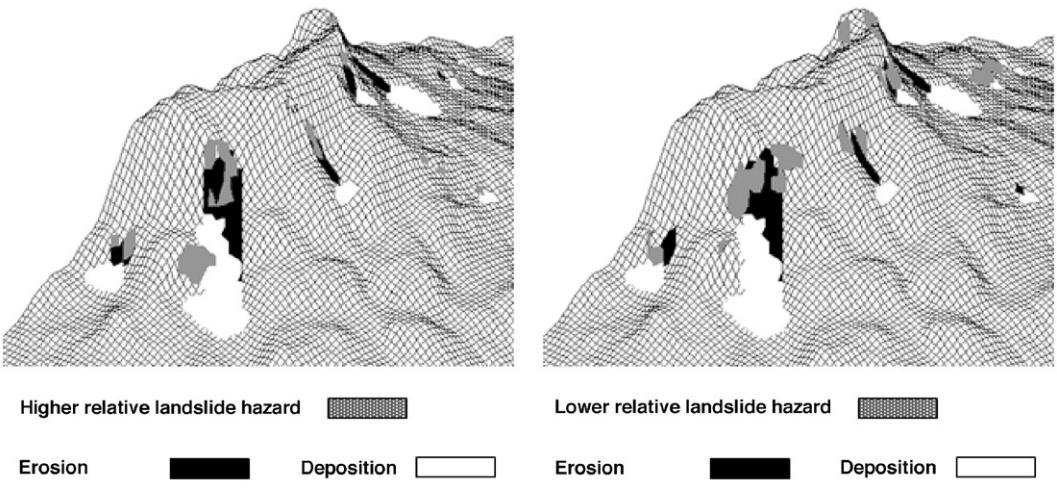

Fig. 7. Comparison of hazard maps between timesteps and visualization of resulting (in)stability patterns.

It should be noted that valid results can only be obtained when the topography of the study area and dimensions of the landslides are well represented by the grid resolution of the digital elevation model used. An elaborate discussion about scale issues and aggregation and disaggregation of spatial data used in landscape process modelling and LAPSUS more specifically can be found in Schoorl et al. (2000). A detailed study on how grid resolution influences the outcome of the proposed landslide model is described in Claessens et al. (2005).

Furthermore, the hypothesis for the present study is that the impact of many rainfall events of different intensity and duration that trigger shallow landslides over a number of years will result in the failure of all sites with a critical steady state rainfall amount below a threshold value during a given timestep. The validity of this hypothesis could be investigated when detailed meteorological data in combination with an inventory of failures triggered by specific rainfall events with a certain intensity and frequency are available.

The overall aim of the model is to assess the spatial impacts of shallow landsliding on longer-term landscape dynamics; it is not the intention to simulate detailed changes in channel geometry or hillslope geomorphology caused by individual failures. Especially the soil redistribution algorithms (Eqs. (9)–(13)) have no true physical basis. To be able to simulate debris flow movement with process-based formulas, a lot of additional parameters would have to be gathered (e.g. viscosity, debris flow composition, soil depth…). On the landscape level, and dealing with long term simulations, these properties would be hard to quantify in a spatially explicit way. The empirical model used in this study does not require this information but can easily incorporate a slope limit on debris flow movement. It takes into account hillslope morphology for erosion and deposition, is based on elevation differences and therefore convenient when basin topography is represented by a digital elevation model. In spite of its assumptions and limitations this approach has been demonstrated to retain the essence of the physical controls of topography and soil properties on landsliding and remains parametrically simple for ease of calibration and application in catchment studies.

4. Conclusions

In this paper we adopt and combine principles and modelling techniques of a physically based slope stability model, a steady state subsurface flow model and debris flow runout criteria. The resulting model forms a landslide component within the dynamic landscape evolution model LAPSUS, which can also simulate soil redistribution by water run-off and tillage erosion. The overall aim of the model component is to assess the impacts of shallow landsliding on longer term landscape dynamics and help to define possible feedbacks with other hillslope processes; it is not the intention to simulate detailed changes in hillslope geomorphology caused by individual shallow landslides. The adopted approach, in combination with field and laboratory measurements, explores the capabilities of the model to calculate relative landslide potentials and visualize the changing pattern of slope instability within a timeframe of years to decades. The model presents a simple and robust method to address the effects of shallow landslide erosion and sedimentation. Digital elevation data are adapted between timesteps and on- and off-site effects over the years can be simulated. The combined infinite slope stability and subsurface flow model performs well in predicting landslide locations with their relative failure potential and is capable of producing results which have a physically realistic interpretation. For determination of debris flow trajectories sophisticated formulations applicable to a well-specified individual debris flow were inappropriate and simpler, empirical formulas were used. Validation of these criteria requires data sets linking landslide events with rainfall conditions triggering their occurrence and their resulting soil redistribution. This is a demanding requirement for large research areas and parameter estimation with resulting uncertainty may therefore be necessary. Improvements of the existing techniques and especially the full integration of all LAPSUS model components are envisaged in the future. Moreover, because the influence of vegetation on soil cohesion is not treated as a spatially lumped parameter input, the model could be used with different land use cover (change) scenarios addressing the impact on landscape development and natural resources. Consequently, the integration of LAPSUS with the existing land use change model CLUE (Verburg et al., 2002) is the subject of future research.

Acknowledgements

The research in New Zealand was supported by the Netherlands Organisation for Scientific Research (NWO) Project 810.62.013 ‘Podzolisation under Kauri (*Agathis australis*): for better or worse?’ The authors gratefully acknowledge T. Van Asch and R. J. Allison for their valuable comments which improved the manuscript. We also wish to thank T. Van Asch and T. Bogaard (Utrecht University) for useful advice and providing the direct

shear test apparatus. Thanks to B. Kempen and W. Thijs for field work assistance. We also would like to thank the Auckland Regional Council, Te Kawerau a Maki and Watercare Ltd. for their support and advice.

References

Ahnert, F., 1987. An approach to the identification of morphoclimates. In: Gardiner, V. (Ed.), International Geomorphology 1986. J. Wiley, Chicester, pp. 159–188.

Auckland Regional Council, 2002. Auckland Water Resource Quantity Statement 2002, TP 171. ARC, Auckland, New Zealand.

Bathurst, J.C., Burton, A., Ward, T.J., 1997. Debris flow run-out and landslide sediment delivery model tests. Journal of Hydraulic Engineering 123 (5), 410–419.

Benda, L.E., Cundy, T.W., 1990. Predicting deposition of debris flows in mountain channels. Canadian Geotechnical Journal 27, 409–417.

Borga, M., Dalla Fontana, G., Da Ros, D., Marchi, L., 1998. Shallow landslide hazard assessment using a physically based model and digital elevation data. Environmental Geology 35 (2–3), 81–88.

Borga, M., Dalla Fontana, G., Gregoretti, C., Marchi, L., 2002. Assessment of shallow landsliding by using a physically based model of hillslope stability. Hydrological Processes 16, 2833–2851.

Brand, E.W., Hudson, R.R., 1982. CHASE — an empirical approach to the design of cut slopes in Hong Kong soils. Proc. 7th S.E. Asian Geotechnical Conf., Hong Kong, vol. 1, pp. 1–16.

Brooks, S.M., Crozier, M.J., Preston, N.J., Anderson, M.G., 2002. Regolith stripping and the control of shallow translational hillslope failure: application of a two-dimensional coupled soil hydrology-slope stability model, Hawke's Bay, New Zealand. Geomorphology 45, 165–179.

Burton, A., Bathurst, J.C., 1998. Physically based modelling of shallow landslide sediment yield at a catchment scale. Environmental Geology 35, 89–99.

Claessens, L., Heuvelink, G.B.M., Schoorl, J.M., Veldkamp, A., 2005. DEM resolution effects on shallow landslide hazard and soil redistribution modelling. Earth Surface Processes and Landforms 30, 461–477.

Claessens, L., Verburg, P.H., Schoorl, J.M., Veldkamp, A., 2006. Contribution of topographically based landslide hazard modelling to the analysis of the spatial distribution and ecology of kauri (Agathis australis). Landscape Ecology 21, 63–76.

Crozier, M.J., 1999. Prediction of rainfall-triggered landslides: a test of the antecedent water status model. Earth Surface Processes and Landforms 24, 825–833.

Denyer, K., Cutting, M., Campbell, G., Green, C., Hilton, M., 1993. Waitakere Ecological District, Survey Report for the Protected Natural Areas Programme. Auckland Regional Council, Newton.

Dietrich, W.E., Wilson, C.J., Montgomery, D.R., McKean, J., Bauer, R., 1992. Erosion thresholds and land surface morphology. Geology 20, 675–679.

Dietrich, W.E., Wilson, C.J., Montgomery, D.R., McKean, J., 1993. Analysis of erosion thresholds, channel networks and landscape morphology using a digital terrain model. Journal of Geology 101, 161–180.

Dietrich, W.E., Reiss, R., Hsu, M., Montgomery, D.R., 1995. A process-based model for colluvial soil depth and shallow landsliding using digital elevation data. Hydrological Processes 9, 383–400.

Douglas, I., 1999. Hydrological investigations of forest disturbance and land cover impacts in South–East Asia: a review. Philosophical Transactions of the Royal Society of London. Series B 354, 1725–1738.

Douglas, I., Bidin, K., Balamurugan, G., Chappell, N.A., Walsh, R.P.D., Greer, T., Sinun, W., 1999. The role of extreme events in the impacts of selective forestry on erosion during harvesting and recovery phases at Danum Valley, Sabah. Philosophical Transactions of the Royal Society of London. Series B 354, 1749–1761.

Dykes, A.P., 2002. Weathering-limited rainfall-triggered shallow mass movements in undisturbed steepland tropical rainforest. Geomorphology 46, 73–93.

Dykes, A.P., Thornes, J.B., 1996. Tectonics and relief in tropical forested mountains: the Gipfelflur hypothesis revisited. In: Anderson, M.G., Brooks, S.M. (Eds.), Advances in Hillslope Processes, vol. 2. Wiley, Chicester, pp. 975–994.

Fannin, R.J., Wise, M.P., 2001. An empirical–statistical model for debris flow travel distance. Canadian Geotechnical Journal 38, 982–994.

FAO, 2001. Lecture Notes on the Major Soils of the World. World Soil Resources Report, vol. 94. FAO, Rome.

Foster, G.R., Meyer, L.D., 1972. A closed-form soil erosion equation for upland areas. In: Shen, H.W. (Ed.), Sedimentation: Symposium to Honour Professor H. A. Einstein. Colorado State University, Fort Collins, Colorado, pp. 12.1–12.19.

Foster, G.R., Meyer, L.D., 1975. Mathematical simulation of upland erosion by fundamental erosion mechanics. In: Anonymous (Ed.), Present and Perspective Technology for Predicting Sediment Yields and Sources. Proceedings Sediment Yield Workshop, Oxford 1972. United States Department of Agriculture, Washington D.C., pp. 190–207.

Graham, J., 1984. Methods of stability analysis. In: Brunsden, D., Prior, D.B. (Eds.), Slope Instability. Wiley Chicester, pp. 171–215.

Guzzetti, F., Carrara, A., Cardinali, M., Reichenbach, P., 1999. Landslide hazard evaluation: a review of current techniques and their application in a multi-scale study, Central Italy. Geomorphology 31, 181–216.

Hayward, B.W., 1976. Lower Miocene stratigraphy and structure of the Waitakere Ranges, North Auckland, New Zealand and the Waitakere Group (new). New Zealand Journal of Geology and Geophysics 19, 871–895.

Hayward, B.W., 1983. Sheet Q11 Waitakere, Geological Map of New Zealand 1:50 000. Map (1 Sheet) and Notes (28 p.). Wellington, New Zealand Department of Scientific and Industrial Research.

Ikeya, H., 1981. A method for designation for area in danger of debris flow. In: Davies, T.R.H., Pearce, A.K. (Eds.), Erosion and Sediment Transport in Pacific Rim Steeplands. Int. Assoc. Hydrol. Sci., Publ., vol. 132, pp. 281–288.

Johnson, A.M., Rodine, J.R., 1984. Debris flow. In: Brunsden, D., Prior, D.B. (Eds.), Slope Instability. Wiley, Chicester, pp. 257–361.

Kessler, J., Oosterbaan, R., 1974. Determining hydraulic conductivities of soils. Drainage Principles and Applications. Publication 16, III, International Institute for Land Reclamation and Improvement. Wageningen, The Netherlands, pp. 253–296.

Kirkby, M.J., 1971. Hillslope process–response models based on the continuity equation. In: Brunsden, D. (Ed.), Slopes, Forms and Processes. Inst. Brit. Geographers, Spec. Pub., pp. 15–30.

Kirkby, M.J., 1987. General models of long-term slope evolution through mass movement. In: Anderson, M.G., Richards, K.S. (Eds.), Slope Stability. Wiley, Chicester, pp. 359–379.

Larsen, M.C., Torres-Sanchez, A.J., 1998. The frequency and distribution of recent landslides in three montane tropical regions of Puerto Rico. Geomorphology 24, 309–331.

Mizuyama, T., Ishikawa, Y., 1990. Prediction of Debris Flow Prone Areas and Damage. American Society of Civil Engineers.

Proceedings of International Symposium Hydraulics/Hydrology of Arid Lands, San Diego, Calif., pp. 712–717.
Mizuyama, T., Yazawa, A., Ido, K., 1987. Computer simulation of debris flow depositional processes. International Association of Hydrological Sciences, Publication 165, 179–190.
Montgomery, D.R., Dietrich, W.E., 1994. A physically based model for the topographic control on shallow landsliding. Water Resources Research 30, 1153–1171.
Montgomery, D.R., Schmidt, K.M., Greenberg, H.M., Dietrich, W.E., 2000. Forest clearing and regional landsliding. Geology 28 (4), 311–314.
Moore, I.D., O'Loughlin, E.M., Burch, G.J., 1988. A contour based topographic model for hydrological and ecological applications. Earth Surface Processes and Landforms 13, 305–320.
Murdoch, G.J., 1991. Cultural Influences on the Ecology of the Waitakere Ranges. ARC Resource management division, Auckland, New Zealand. Unpublished report.
O'Brien, J.S., Fullerton, W.T., 1990. Two-dimensional modeling of alluvial fan flows. American Society of Civil Engineers, Proceedings of International Symposium Hydraulics/Hydrology of Arid Lands, San Diego, Calif. 263–273.
O'Loughlin, E.M., 1986. Prediction of surface saturation zones in natural catchments by topographic analysis. Water Resources Research 22, 794–804.
Pack, R.T., Tarboton, D.G., Goodwin, C.N., 2001. Assessing terrain stability in a GIS using SINMAP. 15th Annual GIS Conference, GIS 2001, British Columbia.
Quinn, P., Beven, K., Chevallier, P., Planchon, O., 1991. The prediction of hillslope flow paths for distributed hydrological modelling using digital terrain models. Hydrological Processes 5, 59–79.
Reid, L.M., Page, M.J., 2003. Magnitude and frequency of landsliding in a large New Zealand catchment. Geomorphology 49, 71–88.
Schoorl, J.M., Veldkamp, A., 2001. Linking land use and landscape process modeling: a case study for the Alora region (South Spain). Agriculture, Ecosystems and Environment 85, 281–292.
Schoorl, J.M., Sonneveld, M.P.W., Veldkamp, A., 2000. Three-dimensional landscape process modeling: the effect of DEM resolution. Earth Surface Processes and Landforms 25, 1025–1043.
Schoorl, J.M., Veldkamp, A., Bouma, J., 2002. Modelling water and soil redistribution in a dynamic landscape context. Soil Science Society of America Journal 66, 1610–1619.
Selby, M., 1993. Hillslope Materials and Processes. Oxford University Press, Oxford.
Takahashi, T., 1991. Debris-Flow. Balkema, Rotterdam.
Van Beek, L.P.H., 2002. The effect of land use and climatic change on slope stability in the Alcoy region (Spain). PhD thesis, Faculty of Geographical Sciences, Utrecht University, The Netherlands.
Van Westen, C.J., 1993. Application of Geographical Information Systems to Landslide Hazard Zonation. ITC Publication, vol. 15. ITC, Enschede, The Netherlands.
Vanacker, V., Vanderschaeghe, M., Govers, G., Willems, E., Poesen, J., Deckers, J., De Bievere, B., 2003. Linking hydrological, infinite slope stability and land-use change models through GIS for assessing the impact of deforestation on slope stability in high Andean watersheds. Geomorphology 52, 299–315.
Vandre, B.C., 1985. Rudd Creek debris flow. In: Bowles, D.S. (Ed.), Delineation of Landslide, Flash Flood, and Debris Flow Hazards in Utah. General Series Rep UWRL/G-85/03. Utah Water Research Laboratory, Utah State University, Logan, Utah, pp. 117–131.
Verburg, P.H., Soepboer, W., Veldkamp, A., Limpiada, R., Espaldon, V., Sharifah Mastura, S.A., 2002. Modeling the spatial dynamics of regional land use: the CLUE-S model. Environmental Management 30 (3), 391–405.
Wu, W., Sidle, R.C., 1995. A distributed slope stability model for steep forested basins. Water Resources Research 31, 2097–2110.